



Static Thin Disks with Power-law Density Profiles*

P. Kotlařík, D. Kofroň, and O. Semerák

Institute of Theoretical Physics, Faculty of Mathematics and Physics, Charles University, Prague, Czech Republic

Received 2022 February 15; revised 2022 March 19; accepted 2022 March 21; published 2022 June 7

Abstract

The task of finding the potential of a thin circular disk with power-law radial density profile is revisited. The result, given in terms of infinite Legendre-type series in the above reference, has now been obtained in closed form thanks to the method of Conway employing Bessel functions. Starting from a closed-form expression for the potential generated by the elementary density term ρ^{2l} , we cover more generic—finite solid or infinite annular—thin disks using superposition and/or inversion with respect to the rim. We check several specific cases against the series-expansion form by numerical evaluation at particular locations. Finally, we add a method to obtain a closed-form solution for *finite* annular disks whose density is of “bump” radial shape, as modeled by a suitable combination of several powers of radius. Density and azimuthal pressure of the disks are illustrated on several plots, together with radial profiles of free circular velocity.

Unified Astronomy Thesaurus concepts: [Relativistic disks \(1388\)](#); [Black holes \(162\)](#)

1. Introduction

Disk sources of gravitation have a clear astrophysical importance. Disk configurations typically result from the combined effect of central attraction—due to a central body or due to the disk itself—and centrifugal force due to orbital motion of the disk matter. In Newton’s theory, the gravitational field is fully represented by potential, given by mass density through the Poisson equation. In general relativity, where mass *currents* also contribute to the field, one has to also specify how the matter *moves*—i.e., how it orbits in the disk case. Unfortunately, when there is some overall net rotation, Einstein equations lead to a difficult problem, usually not solvable by analytical methods. On the other hand, if rotation can be neglected, or if it is compensated as in the case of two equal counter-orbiting streams, the situation is much simpler. More specifically, in the *static* and *axially symmetric* vacuum (or possibly electro-vacuum) case, the gravitational field can always be described by the spacetime metric of the Weyl type¹

$$ds^2 = -e^{2\nu} dt^2 + \rho^2 e^{-2\nu} d\phi^2 + e^{2\lambda-2\nu} (d\rho^2 + dz^2), \quad (1)$$

where t , ρ , ϕ , and z are the Weyl cylindrical coordinates, ν (counterpart of the Newtonian gravitational potential) is given by the Laplace equation (so it behaves linearly), and λ is found (from ν) by quadrature

$$\lambda = \int_{\text{axis}}^{\rho, z} \rho [(\nu_{,\rho}^2 - \nu_{,z}^2) d\rho + 2\nu_{,\rho\nu,z} dz], \quad (2)$$

computed along any path going through the (electro-)vacuum region.

Therefore, the Laplace equation is the key to the external field in Newtonian gravitation, in electrostatics, as well as in *static* general relativity. In the last case, however, the field is *not* in general represented completely by the thus determined potential; in the axially symmetric case, specifically, it also depends on the second metric function λ , which influences the geometry of meridional (ρ , z) sections and which can deviate the whole picture from the Newtonian form significantly. Still, the linearity of the Laplace equation is a tremendous simplification, permitting, in particular, to obtain the field of multicomponent systems by mere superposition. One can thus find, even in general relativity, the field of a static and axisymmetric system of a body encircled by a disk or a ring, as an approximation of, e.g., a black hole surrounded by an accretion disk. Regarding the gravitational dominance of such a compact source as the black hole, the matter in its surroundings is often treated as a test (non-gravitating), but higher (than first) derivatives of the metric/potential are generally prone to subtle effects of “self-gravitation,” and since these are crucial for stability of the motion, the (self-)gravitating matter may sometimes assume a considerably different configuration than the test matter.

The paper is organized as follows. First, we recall in Section 2 how the Poisson integral solution of the Laplace equation appears in the case of a thin circular disk. Following the method suggested by Conway (2000), we then, in Section 3, rewrite that integral in terms of Bessel functions and solve it for a simple power-law density profile. The case of more general power-law (polynomial) density profiles is solved, in a closed form, in Section 4, both for solid and annular disks. In Section 5, the closed-form result is

* Dedicated to our teacher, Professor Jiří Bičák, on the occasion of his 80th birthday. For O.S., Jiří’s interest in thin disks was, 30 yr ago (Bičák et al. 1993), the first motivation to study the topic.

¹ We use the $(-+++)$ signature of the metric, and geometrized units in which $c = 1$, $G = 1$.



numerically checked against the series-expansion solution presented in Semerák (2004). After briefly explaining, in Section 6, why the procedure only works for a density involving even powers of radius, we add in Section 7 how to obtain the potential of a *finite* disk with “bump”-type density profile. Physical properties of the disk sources are illustrated in Sections 8 (radial profiles of density and of azimuthal pressure) and 9 (radial profile of circular-geodesic velocity). Finally, we make several remarks in Section 10, mainly mentioning similar results that have appeared in the literature recently.

2. Static Thin Circular Disks

Computation of the potential of static thin circular disks is a classical problem of the potential theory. In Newton’s theory of gravitation, it is mostly solved while modeling the gravitational field of galactic disks, while in general relativity, one mostly tackles it when modeling accretion disks around compact objects. Although it reduces to the Laplace equation in both theories, in the static case, it remains a challenge, as it is best illustrated by the “trivial” case of uniform surface density when the result still involves elliptic integrals of all three kinds (e.g., Lass & Blitzler 1983). For a thin disk lying in the equatorial plane ($z = 0$), with an outer rim situated on some Weyl radius b , the Poisson integral for ν reads

$$\nu(\rho, z) = -2 \int_0^\pi \int_0^b \frac{w(\rho') \rho' d\rho' d\phi}{\sqrt{\rho^2 + z^2 + \rho'^2 - 2\rho\rho' \cos \phi}}. \quad (3)$$

Integration with respect to ρ' leads to an expression containing Appell’s hypergeometric function of two variables, while that with respect to ϕ yields

$$\nu(\rho, z) = -4 \int_0^b \frac{w(\rho') \rho'}{\sqrt{(\rho + \rho')^2 + z^2}} K\left(\frac{2\sqrt{\rho\rho'}}{\sqrt{(\rho + \rho')^2 + z^2}}\right) d\rho'. \quad (4)$$

On the symmetry axis ($\rho = 0$), it simplifies considerably, because the complete elliptic integral of the first kind $K(k)$ reduces to $\pi/2$. In the axisymmetric case, knowledge of ν on the axis is crucial, since if the latter can be expanded as a power series in z ,

$$\nu(z) = -\frac{\mathcal{M}}{b} \sum_{j=0}^{\infty} \left(\alpha_j \frac{z^j}{b^j} + \beta_j \frac{b^{j+1}}{z^{j+1}} \right), \quad (5)$$

the potential at general location is obtained just by replacing z with $\sqrt{\rho^2 + z^2}$ in the above sum and multiplying each of its terms by the Legendre polynomial $P_j\left(\frac{z}{\sqrt{\rho^2 + z^2}}\right)$. In (5), α_j and β_j are coefficients and \mathcal{M} represents the disk mass in our case.

If interested in *annular* disks rather than in finite solid ones, one can perform an inversion with respect to the rim at $\rho = b$ (also called the Kelvin transformation),

$$\rho \rightarrow \frac{b^2 \rho}{\rho^2 + z^2}, \quad z \rightarrow \frac{b^2 z}{\rho^2 + z^2}; \quad \nu(\rho, z) \rightarrow \frac{b}{\sqrt{\rho^2 + z^2}} \nu\left(\frac{b^2 \rho}{\rho^2 + z^2}, \frac{b^2 z}{\rho^2 + z^2}\right). \quad (6)$$

Actually, such a transformation leaves the solution of the Laplace equation a solution, just that it corresponds then to an annular disk, stretching from $\rho = b$ to radial infinity.

Two additional features are required naturally: the spacetime should be reflection symmetric, so z must appear as $|z|$ in odd powers; and the potential should be finite everywhere, at the origin ($\sqrt{\rho^2 + z^2} = 0$) and at infinity ($\sqrt{\rho^2 + z^2} \rightarrow \infty$) in particular. Anyway, the above recipe yields the result in terms of the Legendre-type series, which is not ideal, due to rather bad convergence properties. A closed-form formula would definitely be more desirable. Unfortunately, such has been found only rarely, because the Poisson integral (4) usually is not elementary. One of the simple exceptions is the Morgan–Morgan family of solutions (Morgan & Morgan 1969), which corresponds, after inversion with respect to the rim, to the surface densities

$$w_{\text{iMM}}^{(m)}(\rho) = \frac{2^{2m} (m!)^2 \mathcal{M} b}{(2m)! \pi^2 \rho^3} \left(1 - \frac{b^2}{\rho^2}\right)^{m-1/2}. \quad (7)$$

The corresponding ν potentials are expressed in terms of *finite* Legendre series (with $m + 1$ terms), so there is no truncation issue. The superposition of the Morgan–Morgan disks with a Schwarzschild-type black hole was studied by, e.g., Lemos & Letelier (1994) and Semerák (2003).

In Semerák (2004), we derived the potentials for similar (also annular) disks with densities of the power-law form

$$w_{\text{i}}^{(m,n)}(\rho) = \binom{m + \frac{1}{n}}{m} \frac{\mathcal{M} b}{2\pi \rho^3} \left(1 - \frac{b^n}{\rho^n}\right)^m, \quad (8)$$

where m and n are natural numbers and the first parenthesis stands for binomial coefficient. These behave somewhat more regularly at the inner rim and do not involve the square root. We were able to find the potential in closed form on the axis, but elsewhere it was

only given in terms of an infinite Legendre sum. The purpose of the present paper is to show that it can be written in a closed form. The key feature will be the relation between a complete elliptic integral of the first kind and an integral over a product of Bessel functions and exponentials.

3. Potential in Terms of the Bessel Functions

The alternative formulation we will build on first appeared within electrodynamics and later was applied to galactic disks by Toomre (1963). More recently, Conway (2000) developed it to obtain closed-form solutions for the potential of matter confined within axisymmetric boundaries. It consists of expressing the axisymmetric Green function, i.e., the potential due to an infinitesimally thin circular loop placed at (ρ', z') , as

$$\nu_{\text{loop}}(\rho, z) = -2\pi\rho' \int_0^\infty J_0(s\rho')J_0(s\rho)e^{-s|z-z'|} ds, \quad (9)$$

where J_0 is the zero-order Bessel function of the first kind and s is an auxiliary real variable. The potential due to a thin source of surface density $w(\rho')$, placed at $z' = 0$, can thus be written as

$$\nu(\rho, z) = -2\pi \int_0^\infty \int_0^\infty \rho' w(\rho') J_0(s\rho') J_0(s\rho) e^{-s|z|} ds d\rho'. \quad (10)$$

The double integration of (10) looks more complicated than the single one in (4), but this is outweighed by having much better knowledge of integrals involving Bessel functions.

3.1. Potential for Power-law Density Terms: Convolution with the Bessel Functions

Consider the density given by an even power of ρ' within some finite radial range $(0, b)$,

$$w(\rho') = (\rho')^{2l}, \quad 0 < \rho' < b, \quad l > 0 \text{ integer.}$$

In such a case, the radial integration in (10) yields

$$\int_0^b \rho' w(\rho') J_0(s\rho') d\rho' = \frac{b^{2l+2}}{2l+2} {}_1F_2\left(1+l; 2+l, 1; -\frac{b^2 s^2}{4}\right), \quad (11)$$

with ${}_1F_2$ the ‘‘1,2’’ generalized hypergeometric function. Employing the contiguous relation

$$c {}_1F_2(a; b+1, c; z) = b {}_1F_2(a; b, c+1; z) - (b-c) {}_1F_2(a; b+1, c+1; z), \quad (12)$$

we can express ${}_1F_2$ in terms of ${}_0F_1$, and thus, thanks to the identity

$${}_1F_2\left(a; a, c; -\frac{z^2}{4}\right) = {}_0F_1\left(-; c; -\frac{z^2}{4}\right) = \left(\frac{z}{2}\right)^{1-c} \Gamma(c) J_{c-1}(z), \quad (13)$$

as a combination of Bessel functions, with a and c integers. In particular, regarding the symmetry ${}_1F_2(a; b, c; z) = {}_1F_2(a; c, b; z)$, we have

$$\begin{aligned} & {}_1F_2\left(1+l; 2+l, 1; -\frac{b^2 s^2}{4}\right) \\ &= \sum_{j=1}^l (-1)^{j+1} \binom{l+1}{j} {}_1F_2\left(1+l; 1+l, j+1; -\frac{b^2 s^2}{4}\right) + (-1)^l {}_1F_2\left(1+l; 2+l, 1+l; -\frac{b^2 s^2}{4}\right) \\ &= (l+1)! \sum_{j=1}^{l+1} \frac{(-1)^{j+1}}{(l+1-j)!} \left(\frac{2}{bs}\right)^j J_j(bs). \end{aligned} \quad (14)$$

Using the above relations, we can write the potential (10) of the power-law density term $w(\rho') = (\rho')^{2l}$ as

$$\nu^{(2l)}(\rho, z) = -\pi \frac{b^{2l+2}}{l+1} \int_0^\infty {}_1F_2\left(1+l; 2+l, 1; -\frac{b^2 s^2}{4}\right) J_0(s\rho) e^{-s|z|} ds = \pi b^{2l+2} l! \sum_{j=1}^{l+1} \frac{(-2)^j}{b^j (l+1-j)!} \mathcal{I}_{(-j, 0)}, \quad (15)$$

where we have denoted

$$\mathcal{I}_{(\alpha,\beta,\gamma)} := \int_0^\infty s^\alpha J_\beta(sb) J_\gamma(s\rho) e^{-s|z|} ds. \quad (16)$$

Conway (2000) studied this kind of ‘‘Bessel–Laplace’’ integral in his Appendix B.² We collect the main results here. The lowest of the integrals can be computed directly (see the Appendix of Conway 2001):³

$$\mathcal{I}_{(0,0,0)} = \frac{kK(k)}{\pi\sqrt{b\rho}}, \quad (17)$$

$$\mathcal{I}_{(0,1,1)} = \frac{1}{\pi k \sqrt{b\rho}} [(2 - k^2)K(k) - 2E(k)], \quad (18)$$

$$\mathcal{I}_{(0,1,0)} = -\frac{k|z|}{2\pi b \sqrt{b\rho}} \left[\frac{b - \rho}{b + \rho} \Pi\left(\frac{4b\rho}{(b + \rho)^2}, k\right) + K(k) \right] + \frac{1}{b} H(b - \rho), \quad (19)$$

where

$$k := \frac{2\sqrt{b\rho}}{\sqrt{(\rho + b)^2 + z^2}} \quad (20)$$

and H is the Heaviside step function. A general $\mathcal{I}_{(\alpha,\beta,\gamma)}$ can be obtained using the recurrence relations⁴

$$\mathcal{I}_{(\alpha,\beta,\gamma)} = \frac{b}{2\beta} [\mathcal{I}_{(\alpha+1,\beta+1,\gamma)} + \mathcal{I}_{(\alpha+1,\beta-1,\gamma)}], \quad (21)$$

$$\mathcal{I}_{(0,\beta,\gamma)} = \frac{2(\gamma + 1)|z|}{(\gamma + 1 - \beta)\rho} \mathcal{I}_{(0,\beta,\gamma+1)} - \frac{2(\gamma + 1)b}{(\gamma + 1 - \beta)\rho} \mathcal{I}_{(0,\beta-1,\gamma+1)} + \frac{\gamma + 1 + \beta}{\gamma + 1 - \beta} \mathcal{I}_{(0,\beta,\gamma+2)}, \quad (22)$$

$$\mathcal{I}_{(0,\gamma+1,\gamma)} = \frac{\rho}{b} \mathcal{I}_{(0,\gamma,\gamma-1)} + \frac{\rho}{2\gamma} [\mathcal{I}_{(1,\gamma+1,\gamma+1)} - \mathcal{I}_{(1,\gamma-1,\gamma-1)}], \quad (23)$$

$$\mathcal{I}_{(1,\gamma,\gamma)} = \frac{(2\gamma - 1)|z|k^2}{8b\rho(1 - k^2)} [k^2 \mathcal{I}_{(0,\gamma-1,\gamma-1)} - (2 - k^2)\mathcal{I}_{(0,\gamma,\gamma)}], \quad (24)$$

$$\mathcal{I}_{(0,\gamma,\gamma)} = \frac{4(\gamma - 1)}{2\gamma - 1} \frac{2 - k^2}{k^2} \mathcal{I}_{(0,\gamma-1,\gamma-1)} - \frac{2\gamma - 3}{2\gamma - 1} \mathcal{I}_{(0,\gamma-2,\gamma-2)} \dots = \frac{1}{\pi\sqrt{b\rho}} Q_{\gamma-1/2}\left(\frac{\rho^2 + b^2 + z^2}{2b\rho}\right) \quad (\gamma > -1/2), \quad (25)$$

where $Q_{\gamma-1/2}$ are Legendre functions of the second kind (toroidal functions).

For our potential formula (15), we first reduce the first index of $\mathcal{I}_{(-j,j,0)}$ to zero using (21) and then also do the same with the remaining indices using (22)–(25) successively. Since $\mathcal{I}_{(0,-1,-1)} = \mathcal{I}_{(0,1,1)}$, one ends up with just a combination of (17)–(19), which means that $\nu^{(2l)}$ is obtained in closed form. However, the procedure grows cumbersome for higher exponents, because the order of the polynomial ‘‘coefficients’’ in front of the resulting elliptic integrals gradually grows. It is thus useful to create, for evaluation of a generic-case potential, a package in some symbolic-manipulation software; we have used Mathematica for that purpose.

Let us illustrate how the result (15) appears in specific cases. For $l = 0$, the density is just constant, which leads to the well-known solution derived by, e.g., Lass & Blitzer (1983):

$$\nu^{(0)}(\rho, z) = 2\pi|z|H(b - \rho) - \frac{4\sqrt{b\rho}}{k} E(k) - \frac{b^2 - \rho^2}{\sqrt{b\rho}} kK(k) - \frac{b - \rho}{b + \rho} \frac{z^2 k}{\sqrt{b\rho}} \Pi\left(\frac{4b\rho}{(b + \rho)^2}, k\right). \quad (26)$$

For $l \geq 1$, the potential can be expressed in a similar but generalized form,⁵

$$\nu^{(2l)}(\rho, z) = 2\pi|z|\mathcal{P}_H^{(2l)} H(b - \rho) - \frac{4\sqrt{b\rho}}{k} \mathcal{P}_E^{(2l)} E(k) - \frac{k}{\sqrt{b\rho}} \mathcal{P}_K^{(2l)} K(k) - \frac{b - \rho}{b + \rho} \frac{z^2 k}{\sqrt{b\rho}} \mathcal{P}_\Pi^{(2l)} \Pi\left(\frac{4b\rho}{(b + \rho)^2}, k\right), \quad (27)$$

² Eason et al. (1955) called them ‘‘Lipschitz–Hankel’’ integrals for products of Bessel functions. They actually represent Laplace transform of products of two Bessel functions—see also Hanson & Puja (1997) and Kausel & Baig (2012) for thorough treatments.

³ Conway writes $\mathcal{I}_{(0,1,0)}$ in terms of the Heuman lambda function, whereas we use its relation to complete elliptic integral of the third kind (Eason et al. 1955)

$$\Lambda_0\left(\arcsin\frac{z}{\sqrt{(b - \rho)^2 + z^2}}, k\right) = \frac{2}{\pi} \frac{|b - \rho|}{b + \rho} \frac{|z|}{\sqrt{(b + \rho)^2 + z^2}} \Pi\left(\frac{4b\rho}{(b + \rho)^2}, k\right) = \frac{1}{\pi} \frac{|b - \rho|}{b + \rho} \frac{k|z|}{\sqrt{b\rho}} \Pi\left(\frac{4b\rho}{(b + \rho)^2}, k\right).$$

⁴ Expressions (B27) (B26), (B23), (B12), and (B7) in Appendix B in Conway (2000).

⁵ The factor $(b^2 - \rho^2)$ is really not present in front of $K(k)$ anymore.

where $\mathcal{P}^{(2l)}$ are polynomials in ρ and z . Generally, $\mathcal{P}^{(2l)}$ are even polynomials of the order $2l$ in the case of $\mathcal{P}_{H,\text{II},E}^{(2l)}$, and of the order $2l + 2$ in the case of $\mathcal{P}_K^{(2l)}$. For the first few cases, the polynomials read

$$\mathcal{P}_{H,\text{II}}^{(2)} = \frac{1}{(1 \cdot 3)^1} (3\rho^2 - 2z^2), \quad (28)$$

$$\mathcal{P}_E^{(2)} = \frac{1}{(1 \cdot 3)^2} (b^2 + 4\rho^2 - 11z^2), \quad (29)$$

$$\mathcal{P}_K^{(2)} = \frac{1}{(1 \cdot 3)^2} (5b^4 - b^2\rho^2 - 4\rho^4 + 4b^2z^2 + 16\rho^2z^2 + 5z^4), \quad (30)$$

$$\mathcal{P}_{H,\text{II}}^{(4)} = \frac{1}{(3 \cdot 5)^1} (15\rho^4 - 40\rho^2z^2 + 8z^4), \quad (31)$$

$$\mathcal{P}_E^{(4)} = \frac{1}{(3 \cdot 5)^2} (9b^4 + 16b^2\rho^2 + 64\rho^4 - 47b^2z^2 - 607\rho^2z^2 + 274z^4), \quad (32)$$

$$\mathcal{P}_K^{(4)} = \frac{1}{(3 \cdot 5)^2} (81b^6 - b^4\rho^2 - 16b^2\rho^4 - 64\rho^6 + 8b^4z^2 + 192b^2\rho^2z^2 + 768\rho^4z^2 - 107b^2z^4 - 267\rho^2z^4 - 154z^6), \quad (33)$$

$$\mathcal{P}_{H,\text{II}}^{(6)} = \frac{1}{(5 \cdot 7)^1} (35\rho^6 - 210\rho^4z^2 + 168\rho^2z^4 - 16z^6), \quad (34)$$

$$\mathcal{P}_E^{(6)} = \frac{1}{(5 \cdot 7)^2} (25b^6 + 36b^4\rho^2 + 64b^2\rho^4 + 256\rho^6 - 107b^4z^2 - 631b^2\rho^2z^2 - 5175\rho^4z^2 + 306b^2z^4 + 8132\rho^2z^4 - 1452z^6), \quad (35)$$

$$\begin{aligned} \mathcal{P}_K^{(6)} = \frac{1}{(5 \cdot 7)^2} & (325b^8 - b^6\rho^2 - 4b^4\rho^4 - 64b^2\rho^6 - 256\rho^8 + 12b^6z^2 + 80b^4\rho^2z^2 + 1536b^2\rho^4z^2 + 6144\rho^6z^2 - 59b^4z^4 \\ & - 2819b^2\rho^2z^4 - 10307\rho^4z^4 + 586b^2z^6 - 800\rho^2z^6 + 892z^8). \end{aligned} \quad (36)$$

Although the expressions show some clear combinatorial-type patterns, we have not been able to arrange them completely in a simple closed formula, so it is better to keep the expanded form.

We may also add that, in the equatorial plane ($z = 0$), the exponential $e^{-s|z|}$ reduces to unity and integral (16) can be expressed in terms of a hypergeometric function as

$$\int_0^\infty s^\alpha J_\beta(sb) J_\gamma(s\rho) ds = \frac{2^\alpha}{\gamma!} \frac{\rho^\gamma}{b^{\alpha+\gamma+1}} \frac{\Gamma\left(\frac{\alpha+\beta+\gamma+1}{2}\right)}{\Gamma\left(\frac{\beta-\alpha-\gamma+1}{2}\right)} {}_2F_1\left(\frac{\alpha-\beta+\gamma+1}{2}, \frac{\alpha+\beta+\gamma+1}{2}; \gamma+1; \frac{\rho^2}{b^2}\right), \quad (37)$$

where it is assumed that $\alpha < 1$, $\alpha + \beta + \gamma + 1 > 0$, and $0 < \rho < b$. (For $\rho > b > 0$, one just swaps $\rho \leftrightarrow b$ in the formula.) We are specifically interested in the case $\alpha = -j$, $\beta = j$, $\gamma = 0$ (yielding $\alpha + \beta + \gamma + 1 = 1$) when the expression reduces to

$$\int_0^\infty s^{-j} J_j(sb) J_0(s\rho) ds = \frac{b^{j-1}}{2^j} \frac{\Gamma\left(\frac{1}{2}\right)}{\Gamma\left(j + \frac{1}{2}\right)} {}_2F_1\left(-j + \frac{1}{2}, \frac{1}{2}; 1; \frac{\rho^2}{b^2}\right) = 2^j b^{j-1} \frac{\Gamma(j)}{\Gamma(2j)} {}_2F_1\left(-j + \frac{1}{2}, \frac{1}{2}; 1; \frac{\rho^2}{b^2}\right). \quad (38)$$

The potential due to the density terms given by *negative* powers of ρ' can be obtained by inversion (6). Under the inversion, our $(\rho')^{2l}$ density and the corresponding potential transform as

$$w(\rho') \equiv (\rho')^{2l} \longrightarrow \frac{b^3}{\rho'^3} w(b^2/\rho') = \frac{b^{3+4l}}{\rho'^{3+2l}}, \quad \nu^{(2l)}(\rho, z) \longrightarrow \frac{b}{\sqrt{\rho^2 + z^2}} \nu^{(2l)}\left(\frac{b^2\rho}{\rho^2 + z^2}, \frac{b^2z}{\rho^2 + z^2}\right), \quad (39)$$

hence the density–potential pair

$$w(\rho') = (\rho')^{-3-2l}, \quad \nu_i^{(-3-2l)}(\rho, z) = \frac{b^{-2-4l}}{\sqrt{\rho^2 + z^2}} \nu^{(2l)}\left(\frac{b^2\rho}{\rho^2 + z^2}, \frac{b^2z}{\rho^2 + z^2}\right). \quad (40)$$

More explicitly, the inverted potentials read

$$\begin{aligned} b^{4l} \nu_i^{(-3-2l)}(\rho, z) = & \frac{2\pi|z| \widetilde{\mathcal{P}}_H^{(2l)}}{(\rho^2 + z^2)^{3/2}} H\left(b - \frac{b^2\rho}{\rho^2 + z^2}\right) - \frac{4\sqrt{b\rho}}{bk} \frac{\widetilde{\mathcal{P}}_E^{(2l)} E(k)}{\rho^2 + z^2} - \frac{k \widetilde{\mathcal{P}}_K^{(2l)} K(k)}{b^3 \sqrt{b\rho}} \\ & - \frac{\rho^2 - b\rho + z^2}{\rho^2 + b\rho + z^2} \frac{bz^2k \widetilde{\mathcal{P}}_{\text{II}}^{(2l)}}{(\rho^2 + z^2)^2 \sqrt{b\rho}} \Pi\left(\frac{4b\rho(\rho^2 + z^2)}{(\rho^2 + b\rho + z^2)^2}, k\right), \end{aligned} \quad (41)$$

where $\widetilde{\mathcal{P}}^{(2l)}$ denote the respective polynomials $\mathcal{P}^{(2l)}$ “inverted” according to (6); modulus k of the elliptic integrals is invariant under the inversion, so it keeps the same form (20). Note that we distinguish the inverted potentials by “i,” as opposed to the density w whose character is apparent. Note also that the potentials do not yet have the correct dimension—rather than being dimensionless,

$\nu^{(2l)}$ has the dimension [length] $^{2l+1}$ while $\nu_1^{(-3-2l)}$ has the dimension [length] $^{-2l-2}$.

4. Circular Disks with Generic Power-law Densities

Due to the linearity of the Laplace equation, one can now obtain disk solutions with various power-law radial profiles of density $w(\rho')$ by superposition of elementary terms discussed above. Consider a circular thin disk extending from the center to some finite radius $\rho' = b$, with surface density given by an even polynomial in the radial coordinate,

$$w^{(m,2l)}(\rho') = W \left(1 - \frac{\rho'^{2l}}{b^{2l}}\right)^m, \quad W = \binom{m + \frac{1}{l}}{m} \frac{\mathcal{M}}{\pi b^2}, \quad (42)$$

where l and m are natural numbers and W is a normalization factor ensuring that the disk has the prescribed total mass \mathcal{M} . The radial integration in (10) can, for such a density, be performed using binomial expansion (similarly as Conway 2000 did for $l = 1$), to obtain

$$\begin{aligned} \nu^{(m,2l)}(\rho, z) &= -2\pi W \int_0^\infty \int_0^b \rho' \left(1 - \frac{\rho'^{2l}}{b^{2l}}\right)^m J_0(s\rho') J_0(s\rho) e^{-s|z|} d\rho' ds \\ &= -2\pi W \sum_{q=0}^m \binom{m}{q} \frac{(-1)^q}{b^{2lq}} \int_0^\infty \int_0^b (\rho')^{2lq+1} J_0(s\rho') J_0(s\rho) e^{-s|z|} d\rho' ds \equiv W \sum_{q=0}^m \binom{m}{q} \frac{(-1)^q}{b^{2lq}} \nu^{(2lq)}(\rho, z) \\ &= -\pi W b^2 \sum_{q=0}^m \binom{m}{q} \frac{(-1)^q}{1+lq} \int_0^\infty {}_1F_2\left(1+lq; 2+lq, 1; -\frac{b^2 s^2}{4}\right) J_0(s\rho) e^{-s|z|} ds \\ &\equiv \pi W b^2 \sum_{q=0}^m \binom{m}{q} (-1)^q (lq)! \sum_{j=1}^{lq+1} \frac{(-2)^j}{b^j (lq+1-j)!} \mathcal{I}_{(-j,0)} \\ &= \frac{W}{b^{2lm}} \left[2\pi |z| \mathcal{P}_{H,E,\Pi}^{(m,2l)} H(b-\rho) - \frac{4\sqrt{b\rho}}{k} \mathcal{P}_E^{(m,2l)} E(k) - \frac{k}{\sqrt{b\rho}} \mathcal{P}_K^{(m,2l)} K(k) - \frac{b-\rho}{b+\rho} \frac{z^2 k}{\sqrt{b\rho}} \mathcal{P}_{\Pi}^{(m,2l)} \Pi\left(\frac{4b\rho}{(b+\rho)^2}, k\right) \right], \quad (43) \end{aligned}$$

where $\mathcal{P}_{H,E,\Pi}^{(m,2l)}$ are polynomials (in ρ and z) of the order $2lm$ while $\mathcal{P}_K^{(m,2l)}$ are polynomials of the order $2lm+2$. They are simply related to those obtained for the $(\rho')^{2l}$ density terms in (28)–(36),

$$\mathcal{P}_{H,\Pi}^{(1,2)} = b^2 - \mathcal{P}_{H,\Pi}^{(2)}, \quad \mathcal{P}_E^{(1,2)} = b^2 - \mathcal{P}_E^{(2)}, \quad \mathcal{P}_K^{(1,2)} = b^2(b^2 - \rho^2) - \mathcal{P}_K^{(2)}, \quad (44)$$

$$\mathcal{P}_{H,\Pi}^{(1,4)} = b^4 - \mathcal{P}_{H,\Pi}^{(4)}, \quad \mathcal{P}_E^{(1,4)} = b^4 - \mathcal{P}_E^{(4)}, \quad \mathcal{P}_K^{(1,4)} = b^4(b^2 - \rho^2) - \mathcal{P}_K^{(4)}, \quad (45)$$

$$\mathcal{P}_{H,\Pi}^{(1,6)} = b^6 - \mathcal{P}_{H,\Pi}^{(6)}, \quad \mathcal{P}_E^{(1,6)} = b^6 - \mathcal{P}_E^{(6)}, \quad \mathcal{P}_K^{(1,6)} = b^6(b^2 - \rho^2) - \mathcal{P}_K^{(6)}, \quad (46)$$

$$\mathcal{P}_{H,\Pi}^{(2,2)} = b^4 + \mathcal{P}_{H,\Pi}^{(4)} - 2b^2 \mathcal{P}_{H,\Pi}^{(2)}, \quad \mathcal{P}_E^{(2,2)} = b^4 + \mathcal{P}_E^{(4)} - 2b^2 \mathcal{P}_E^{(2)}, \quad \mathcal{P}_K^{(2,2)} = b^4(b^2 - \rho^2) + \mathcal{P}_K^{(4)} - 2b^2 \mathcal{P}_K^{(2)}, \quad (47)$$

$$\mathcal{P}_{H,\Pi}^{(3,2)} = b^6 - \mathcal{P}_{H,\Pi}^{(6)} + 3b^2 \mathcal{P}_{H,\Pi}^{(4)} - 3b^4 \mathcal{P}_{H,\Pi}^{(2)}, \quad (48)$$

$$\mathcal{P}_E^{(3,2)} = b^6 - \mathcal{P}_E^{(6)} + 3b^2 \mathcal{P}_E^{(4)} - 3b^4 \mathcal{P}_E^{(2)}, \quad (49)$$

$$\mathcal{P}_K^{(3,2)} = b^6(b^2 - \rho^2) - \mathcal{P}_K^{(6)} + 3b^2 \mathcal{P}_K^{(4)} - 3b^4 \mathcal{P}_K^{(2)}. \quad (50)$$

Actually, from the expression $\nu^{(m,2l)}(\rho, z) = W \sum_{q=0}^m \binom{m}{q} \frac{(-1)^q}{b^{2lq}} \nu^{(2lq)}(\rho, z)$, we can summarize the above relations as

$$\mathcal{P}_{H,\Pi,E}^{(m,2l)} = b^{2ml} + \sum_{q=1}^m (-1)^q \binom{m}{q} b^{2l(m-q)} \mathcal{P}_{H,\Pi,E}^{(2lq)}, \quad \mathcal{P}_K^{(m,2l)} = b^{2ml}(b^2 - \rho^2) + \sum_{q=1}^m (-1)^q \binom{m}{q} b^{2l(m-q)} \mathcal{P}_K^{(2lq)}. \quad (51)$$

4.1. The Case of Annular Disks

Annular circular disks are again obtained by inversion (39). Substituting the inverted density

$$w_1^{(m,2l)}(\rho') = \frac{b^3}{\rho'^3} w^{(m,2l)}(b^2/\rho') = W \frac{b^3}{\rho'^3} \left(1 - \frac{b^{2l}}{\rho'^{2l}}\right)^m$$

with W set at

$$W = \binom{m + \frac{1}{2l}}{m} \frac{\mathcal{M}}{2\pi b^2}$$

in order for the total mass of the disk to come out \mathcal{M} (i.e., in the same manner as in (8)),

$$2\pi \int_b^\infty \rho' w_i^{(m,2l)}(\rho') d\rho' = \left(\frac{m + \frac{1}{2l}}{m} \right) \mathcal{M} b \int_b^\infty \frac{1}{\rho'^2} \left(1 - \frac{b^{2l}}{\rho'^{2l}} \right)^m d\rho' = \mathcal{M},$$

we obtain the potential

$$\nu_i^{(m,2l)}(\rho, z) = - \left(\frac{m + \frac{1}{2l}}{m} \right) \frac{m! \mathcal{M} b}{\sqrt{\rho^2 + z^2}} \sum_{q=0}^m \frac{(lq)!}{(m-q)! q!} \sum_{j=1}^{lq+1} \frac{(-1)^{q+j+1} 2^{j-1}}{b^j (lq+1-j)!} \tilde{\mathcal{I}}_{(-j,j,0)}, \quad (52)$$

which, for $l, m \geq 1$, reads more explicitly

$$\begin{aligned} \nu_i^{(m,2l)}(\rho, z) = & \left(\frac{m + \frac{1}{2l}}{m} \right) \frac{\mathcal{M}}{2\pi b^{2ml}} \left[\frac{2\pi b |z|}{(\rho^2 + z^2)^{3/2}} \tilde{\mathcal{P}}_H^{(m,2l)} H\left(b - \frac{b^2 \rho}{\rho^2 + z^2}\right) - \frac{4\sqrt{b\rho}}{k(\rho^2 + z^2)} \tilde{\mathcal{P}}_E^{(m,2l)} E(k) - \frac{k \tilde{\mathcal{P}}_K^{(m,2l)}}{b^2 \sqrt{b\rho}} K(k) \right. \\ & \left. - \frac{\rho^2 - b\rho + z^2}{\rho^2 + b\rho + z^2} \frac{b^2 z^2 k}{(\rho^2 + z^2)^2 \sqrt{b\rho}} \tilde{\mathcal{P}}_\Pi^{(m,2l)} \Pi\left(\frac{4b\rho(\rho^2 + z^2)}{(\rho^2 + b\rho + z^2)^2}, k\right) \right]. \quad (53) \end{aligned}$$

We have denoted by $\tilde{\mathcal{I}}_{(-j,j,0)}$ and $\tilde{\mathcal{P}}^{(m,2l)}$ the respective integrals $\mathcal{I}_{(-j,j,0)}$ and polynomials $\mathcal{P}^{(m,2l)}$ “inverted” according to (6); modulus k of the elliptic integrals is invariant under the inversion, so it keeps the same form (20). The above potential already is dimensionless, as it should be.

Below, we illustrate that the solution is the same as the one given, in the form of multipole expansion, in Semerák (2004), for even n ($\equiv 2l$).

4.2. Behavior of the Potential at Significant Locations

On the axis ($\rho = 0$), we have $k = 0$, so all the elliptic integrals reduce to $\pi/2$, and $H(b) = 1$, which yields

$$\nu_i^{(m,2l)}(z) = \left(\frac{m + \frac{1}{2l}}{m} \right) \frac{\mathcal{M}}{2b^{2ml} z^2} \left[2b \tilde{\mathcal{P}}_H^{(m,2l)} - \sqrt{b^2 + z^2} \tilde{\mathcal{P}}_E^{(m,2l)} - \frac{z^2}{b^2 \sqrt{b^2 + z^2}} \tilde{\mathcal{P}}_K^{(m,2l)} - \frac{b^2}{\sqrt{b^2 + z^2}} \tilde{\mathcal{P}}_\Pi^{(m,2l)} \right]. \quad (54)$$

An explicit result is obtained by substituting for $\tilde{\mathcal{P}}$ s, which means computing the respective polynomials $\mathcal{P}^{(m,2l)}(\rho = 0)$ and performing their inversion, which for $\rho = 0$ reduces to the change of $z \rightarrow b^2/z$. Using computer algebra, one checks that it really equals the formula

$$\nu_i^{(m,n)}(z) = - \left(\frac{m + \frac{1}{n}}{m} \right) \frac{\mathcal{M}}{\sqrt{b^2 + z^2}} \sum_{q=0}^m \frac{(-1)^q}{qn + 2} \binom{m}{q} {}_2F_1\left(\frac{1}{2}, 1; 2 + \frac{qn}{2}; \frac{1}{1 + b^2/z^2}\right) \quad (55)$$

given by Semerák (2004). Especially at the very center, ($\rho = 0, z = 0$), the potential amounts to

$$\nu_i^{(m,n)}(0, 0) = - \frac{\mathcal{M}}{b} \frac{\Gamma(m+1+1/n)\Gamma(2/n)}{\Gamma(m+1+2/n)\Gamma(1/n)}.$$

This increases with m , whereas it decreases with n .

In the plane of the disk ($z = 0$), we were only able in Semerák (2004) to give the potential as an infinite series at $\rho > b$ (i.e., “within” the disk), while in the empty region in the disk center, we wrote

$$\nu_i^{(m,n)}(\rho < b) = - \left(\frac{m + \frac{1}{n}}{m} \right) \frac{\mathcal{M}}{b} \sum_{q=0}^m \frac{(-1)^q}{qn + 2} \binom{m}{q} {}_3F_2\left(\frac{1}{2}, \frac{1}{2}, 1 + \frac{qn}{2}; 1, 2 + \frac{qn}{2}; \frac{\rho^2}{b^2}\right),$$

where ${}_3F_2$ is the generalized hypergeometric function. Now we newly obtain, from (53), the equatorial expression

$$\nu_i^{(m,2l)}(\rho) = - \left(\frac{m + \frac{1}{2l}}{m} \right) \frac{\mathcal{M}}{\pi b^{2ml}} \left[\frac{\rho + b}{\rho^2} \tilde{\mathcal{P}}_E^{(m,2l)} E(k) + \frac{\tilde{\mathcal{P}}_K^{(m,2l)} K(k)}{b^2(\rho + b)} \right]$$

valid both above and below the disk rim. At the very rim, $\rho = b$, both formulae simplify in an obvious manner. In particular, the first one then involves the unity-argument ${}_3F_2$ function, ${}_3F_2\left(\frac{1}{2}, \frac{1}{2}, 1 + \frac{qn}{2}; 1, 2 + \frac{qn}{2}; 1\right)$, which is commonly discussed in the special-function literature. It may be worth noting that, in the even- n case, $n = 2l$, it can be expressed in the closed form (called Ramanujan’s

formula)

$${}_3F_2\left(\frac{1}{2}, \frac{1}{2}, 1 + ql; 1, 2 + ql; 1\right) = \frac{4}{\pi} \frac{1 + ql}{(1 + 2ql)^2} \frac{16^{ql}}{\binom{2ql}{ql}^2} \sum_{j=0}^{ql} \frac{\binom{2j}{j}^2}{16^j}.$$

In the second, elliptic-integral formula, one has (at the disk rim) $k = 1$, which is the singularity of $K(k)$, but since the respective polynomial $\widetilde{\mathcal{P}}_K^{(m,2l)}$ always contains the factor $(\rho^2 - b^2)^2$ in the equatorial plane, the K -term is actually eliminated at the rim and one is left there with

$$\nu_i^{(m,2l)}(\rho = b, z = 0) = -\binom{m + \frac{1}{2l}}{m} \frac{2\mathcal{M}}{\pi b^{2ml+1}} \widetilde{\mathcal{P}}_E^{(m,2l)}.$$

Several first values read, at the rim ($\rho = b, z = 0$),

$$\nu_i^{(1,2)} = -\frac{4}{3} \frac{\mathcal{M}}{\pi b}, \quad \nu_i^{(2,2)} = -\frac{16}{15} \frac{\mathcal{M}}{\pi b}, \quad \nu_i^{(3,2)} = -\frac{32}{35} \frac{\mathcal{M}}{\pi b}, \quad \nu_i^{(1,4)} = -\frac{68}{45} \frac{\mathcal{M}}{\pi b}, \quad \nu_i^{(1,6)} = -\frac{844}{525} \frac{\mathcal{M}}{\pi b}.$$

At radial infinity, the potential falls off as $-\mathcal{M}/\sqrt{\rho^2 + z^2}$, which just confirms the meaning of \mathcal{M} .

5. Numerical Check of the Closed-form Formulae against Series Expansion

A closed-form solution has clear advantages over the series expansion, the more that the Legendre-type series do not tend to converge safely. It is natural to compare the two solutions now, in order to support the reliability of both.

In Tables 1–3, we numerically compare several examples of the annular-disk potential (53) with the solution expressed in term of the multipole expansion in Semerák (2004) (Equations (10) and (11) there). The main message of the tables is that the solutions are really identical. The second observation is that the series expansion converges quite well even at radii close to that of the disk rim, mainly for higher m and lower $2l$, for which the density falls off (or rises) less steeply at the disk edge, making the field more regular.

6. Trouble with Odd Powers of Radius in Density

Up to now, we have been able to employ Conway's method and reach the closed-form solution for even $n (= 2l)$ in the density prescription (8). However, the odd-exponent case, $n = 2l + 1$, is more difficult, as already noticed in Semerák (2004) (the presence of logarithmic terms hindered the standard way of extending the axial result to a generic location). The integration over the source (43) in that case yields

$$\begin{aligned} \int_0^b \rho' \left(1 - \frac{\rho'^{2l+1}}{b^{2l+1}}\right)^m J_0(s\rho') d\rho' &= \sum_{q=0}^m \binom{m}{q} \frac{(-1)^q}{b^{(2l+1)q}} \int_0^b \rho'^{(2l+1)q+1} J_0(s\rho') d\rho' \\ &= \sum_{q=0}^m \binom{m}{q} \frac{(-1)^q b^2}{2 + (2l + 1)q} {}_1F_2\left(1 + lq + \frac{q}{2}; 2 + lq + \frac{q}{2}, 1; -\frac{b^2 s^2}{4}\right). \end{aligned} \quad (56)$$

Here, the contiguous relation (12) does not always work, because the difference between the first and the third parameter of the above ${}_1F_2$ is only an integer for an even q , which means that for odd q the counterpart of (14) would generally be an *infinite* sum.

7. Finite Disks with Bump-type Density Profiles

Finally, we derive, in a closed form as well, the potential of a *finite* annular disk. The respective density profile can be composed, within a selected radial range ($\rho_{\text{in}}, \rho_{\text{out}}$), of the constant-density case plus the $l = 0, 1, 2, \dots, L$ (with $L \geq 1$) sum of the (40) terms. Let us illustrate the recipe on the simplest, $L = 1$ case. Consider, for $\rho_{\text{in}} \leq \rho' \leq \rho_{\text{out}}$, the density

$$w(\rho') = -W_0 + \frac{W_{-3}}{\rho'^3} - \frac{W_{-5}}{\rho'^5}, \quad \text{with} \quad W_{-3} = W_0 \frac{\rho_{\text{out}}^5 - \rho_{\text{in}}^5}{\rho_{\text{out}}^2 - \rho_{\text{in}}^2}, \quad W_{-5} = W_0 \rho_{\text{in}}^2 \rho_{\text{out}}^2 \frac{\rho_{\text{out}}^3 - \rho_{\text{in}}^3}{\rho_{\text{out}}^2 - \rho_{\text{in}}^2}. \quad (57)$$

Table 1
Comparison between the Annular-disk Potential Computed in Closed Form (“Exact” Column) and in Multipole Expansion in the Vicinity of the Disk Rim

$m = 1, 2l = 2$		Number of Summed Terms					
ρ	z	5	10	20	30	50	exact
4.80	-0.10	-0.0817932	-0.0831299	-0.0836179	-0.0837455	-0.0836892	-0.0834522
4.88		-0.0826293	-0.0836648	-0.0839682	-0.0840259	-0.0840193	-0.0839459
4.96		-0.0834771	-0.0842840	-0.0844754	-0.0845019	-0.0845023	-0.0844883
5.04		-0.0843199	-0.0849521	-0.0850746	-0.0850870	-0.0850877	-0.0850859
5.12		-0.0851449	-0.0856429	-0.0857223	-0.0857282	-0.0857285	-0.0857283
5.20		-0.0859424	-0.0863368	-0.0863888	-0.0863916	-0.0863918	-0.0863917
<hr/>							
4.80	-0.05	-0.0815217	-0.0829155	-0.0834898	-0.0837177	-0.0840046	-0.0834822
4.88		-0.0824742	-0.0835518	-0.0839048	-0.0840036	-0.0840816	-0.0839843
4.96		-0.0834240	-0.0842621	-0.0844825	-0.0845263	-0.0845487	-0.0845434
5.04		-0.0843561	-0.0850117	-0.0851513	-0.0851712	-0.0851779	-0.0851784
5.12		-0.0852591	-0.0857746	-0.0858644	-0.0858735	-0.0858756	-0.0858758
5.20		-0.0861245	-0.0865321	-0.0865905	-0.0865948	-0.0865955	-0.0865955
<hr/>							
4.80	0	-0.0812375	-0.0826507	-0.0832549	-0.0835202	-0.0839615	-0.0834923
4.88		-0.0823142	-0.0834060	-0.0837762	-0.0838902	-0.0840054	-0.0839975
4.96		-0.0833721	-0.0842207	-0.0844512	-0.0845013	-0.0845332	-0.0845639
5.04		-0.0843981	-0.0850615	-0.0852072	-0.0852297	-0.0852390	-0.0852417
5.12		-0.0853826	-0.0859041	-0.0859974	-0.0860077	-0.0860106	-0.0860109
5.20		-0.0863186	-0.0867307	-0.0867912	-0.0867961	-0.0867970	-0.0867970
<hr/>							
4.80	0.05	-0.0815217	-0.0829155	-0.0834898	-0.0837177	-0.0840046	-0.0834822
4.88		-0.0824742	-0.0835518	-0.0839048	-0.0840036	-0.0840816	-0.0839843
4.96		-0.0834240	-0.0842621	-0.0844825	-0.0845263	-0.0845487	-0.0845434
5.04		-0.0843561	-0.0850117	-0.0851513	-0.0851712	-0.0851779	-0.0851784
5.12		-0.0852591	-0.0857746	-0.0858644	-0.0858735	-0.0858756	-0.0858758
5.20		-0.0861245	-0.0865321	-0.0865905	-0.0865948	-0.0865955	-0.0865955
<hr/>							
4.80	0.10	-0.0817932	-0.0831299	-0.0836179	-0.0837455	-0.0836892	-0.0834522
4.88		-0.0826293	-0.0836648	-0.0839682	-0.0840259	-0.0840193	-0.0839459
4.96		-0.0834771	-0.0842840	-0.0844754	-0.0845019	-0.0845023	-0.0844883
5.04		-0.0843199	-0.0849521	-0.0850746	-0.0850870	-0.0850877	-0.0850859
5.12		-0.0851449	-0.0856429	-0.0857223	-0.0857282	-0.0857285	-0.0857283
5.20		-0.0859424	-0.0863368	-0.0863888	-0.0863916	-0.0863918	-0.0863917

Note. The disk parameters are $z = 0$, $b = 5\mathcal{M}$, $2l = 2$, and $m = 1$. Coordinates ρ and z are given in units of \mathcal{M} , while the potential values are dimensionless.

Such a combination of powers together yields a fairly reasonable “bump”-type profile. Since the total mass comes out

$$\begin{aligned} \mathcal{M} &\equiv 2\pi \int_{\rho_{\text{in}}}^{\rho_{\text{out}}} \rho' w(\rho') d\rho' = 2\pi W_0 \int_{\rho_{\text{in}}}^{\rho_{\text{out}}} \left(-\rho' + \frac{1}{\rho'^2} \frac{\rho_{\text{out}}^5 - \rho_{\text{in}}^5}{\rho_{\text{out}}^2 - \rho_{\text{in}}^2} - \frac{\rho_{\text{in}}^2 \rho_{\text{out}}^2}{\rho'^4} \frac{\rho_{\text{out}}^3 - \rho_{\text{in}}^3}{\rho_{\text{out}}^2 - \rho_{\text{in}}^2} \right) d\rho' \\ &= \pi W_0 \frac{(\rho_{\text{out}} - \rho_{\text{in}})^3 (4\rho_{\text{in}}^2 + 7\rho_{\text{in}}\rho_{\text{out}} + 4\rho_{\text{out}}^2)}{3\rho_{\text{in}}\rho_{\text{out}}(\rho_{\text{in}} + \rho_{\text{out}})}, \end{aligned}$$

the absolute factor W_0 should be chosen as

$$W_0 = \frac{3\mathcal{M} \rho_{\text{in}}\rho_{\text{out}}(\rho_{\text{in}} + \rho_{\text{out}})}{\pi(\rho_{\text{out}} - \rho_{\text{in}})^3 (4\rho_{\text{in}}^2 + 7\rho_{\text{in}}\rho_{\text{out}} + 4\rho_{\text{out}}^2)}.$$

The potential of the disk follows by subtraction

$$\nu(\rho, z; b = \rho_{\text{out}}) - \nu(\rho, z; b = \rho_{\text{in}}), \quad \text{with} \quad \nu(\rho, z) = -W_0 \nu^{(0)} + W_{-3} \nu_i^{(-3)} - W_{-5} \nu_i^{(-5)}, \quad (58)$$

where $\nu^{(0)}$ is given by (26) and $\nu_i^{(-3)}, \nu_i^{(-5)}$ are given by (41) for $l = 0, 1$. The density and potential of this type of disk are illustrated in Figure 1.

Higher bump-type disks can be constructed in a similar way. In general, one takes certain $L \geq 1$ and $\rho_{\text{out}} > \rho_{\text{in}} > 0$, considers (within the interval $\rho_{\text{in}} \leq \rho' \leq \rho_{\text{out}}$) the density

$$w(\rho') = -W_0 + \sum_{l=0}^L (-1)^l \frac{W_{-3-2l}}{(\rho')^{3+2l}},$$

Table 2
The Same Comparison as in Table 1, but for the Disk with $2l = 2$, $m = 2$ (Top Table) and $2l = 2$, $m = 3$ (Bottom Table)

$m = 2, 2l = 2$		Number of Summed Terms					
ρ	z	5	10	20	30	50	Exact
4.80	-0.10	-0.0681220	-0.0673768	-0.0672671	-0.0672524	-0.0672551	-0.0672715
4.88		-0.0681614	-0.0675781	-0.0675086	-0.0675019	-0.0675021	-0.0675059
4.96		-0.0682612	-0.0678022	-0.0677576	-0.0677545	-0.0677544	-0.0677550
5.04		-0.0684146	-0.0680515	-0.0680225	-0.0680211	-0.0680210	-0.0680211
5.12		-0.0686144	-0.0683259	-0.0683068	-0.0683061	-0.0683061	-0.0683061
5.20		-0.0688538	-0.0686233	-0.0686107	-0.0686103	-0.0686103	-0.0686103
4.80	-0.05	-0.0682020	-0.0674278	-0.0673005	-0.0672748	-0.0672552	-0.0672815
4.88		-0.0682156	-0.0676106	-0.0675308	-0.0675195	-0.0675140	-0.0675172
4.96		-0.0683011	-0.0678258	-0.0677751	-0.0677700	-0.0677684	-0.0677684
5.04		-0.0684493	-0.0680739	-0.0680412	-0.0680389	-0.0680384	-0.0680384
5.12		-0.0686508	-0.0683529	-0.0683315	-0.0683305	-0.0683303	-0.0683303
5.20		-0.0688970	-0.0686594	-0.0686453	-0.0686448	-0.0686448	-0.0686448
4.80	0	-0.0682504	-0.0674663	-0.0673330	-0.0673033	-0.0672737	-0.0672848
4.88		-0.0682413	-0.0676290	-0.0675456	-0.0675327	-0.0675247	-0.0675211
4.96		-0.0683159	-0.0678351	-0.0677822	-0.0677765	-0.0677742	-0.0677730
5.04		-0.0684620	-0.0680825	-0.0680485	-0.0680459	-0.0680452	-0.0680451
5.12		-0.0686684	-0.0683673	-0.0683452	-0.0683439	-0.0683437	-0.0683437
5.20		-0.0689244	-0.0686844	-0.0686698	-0.0686693	-0.0686692	-0.0686692
4.80	0.05	-0.0682020	-0.0674278	-0.0673005	-0.0672748	-0.0672552	-0.0672815
4.88		-0.0682156	-0.0676106	-0.0675308	-0.0675195	-0.0675140	-0.0675172
4.96		-0.0683011	-0.0678258	-0.0677751	-0.0677700	-0.0677684	-0.0677684
5.04		-0.0684493	-0.0680739	-0.0680412	-0.0680389	-0.0680384	-0.0680384
5.12		-0.0686508	-0.0683529	-0.0683315	-0.0683305	-0.0683303	-0.0683303
5.20		-0.0688970	-0.0686594	-0.0686453	-0.0686448	-0.0686448	-0.0686448
4.80	0.10	-0.0681220	-0.0673768	-0.0672671	-0.0672524	-0.0672551	-0.0672715
4.88		-0.0681614	-0.0675781	-0.0675086	-0.0675019	-0.0675021	-0.0675059
4.96		-0.0682612	-0.0678022	-0.0677576	-0.0677545	-0.0677544	-0.0677550
5.04		-0.0684146	-0.0680515	-0.0680225	-0.0680211	-0.0680210	-0.0680211
5.12		-0.0686144	-0.0683259	-0.0683068	-0.0683061	-0.0683061	-0.0683061
5.20		-0.0688538	-0.0686233	-0.0686107	-0.0686103	-0.0686103	-0.0686103
$m = 3, 2l = 2$		Number of Summed Terms					
ρ	z	5	10	20	30	50	Exact
4.80	-0.10	-0.0569667	-0.0577922	-0.0578323	-0.0578348	-0.0578347	-0.0578333
4.88		-0.0572943	-0.0579470	-0.0579729	-0.0579741	-0.0579741	-0.0579738
4.96		-0.0575848	-0.0581035	-0.0581204	-0.0581209	-0.0581209	-0.0581209
5.04		-0.0578497	-0.0582638	-0.0582749	-0.0582752	-0.0582752	-0.0582752
5.12		-0.0580979	-0.0584299	-0.0584373	-0.0584375	-0.0584375	-0.0584375
5.20		-0.0583363	-0.0586036	-0.0586086	-0.0586086	-0.0586086	-0.0586086
4.80	-0.05	-0.0569329	-0.0577875	-0.0578335	-0.0578378	-0.0578398	-0.0578382
4.88		-0.0572725	-0.0579474	-0.0579767	-0.0579787	-0.0579792	-0.0579791
4.96		-0.0575711	-0.0581066	-0.0581256	-0.0581265	-0.0581267	-0.0581267
5.04		-0.0578418	-0.0582688	-0.0582812	-0.0582816	-0.0582817	-0.0582817
5.12		-0.0580948	-0.0584367	-0.0584449	-0.0584451	-0.0584451	-0.0584451
5.20		-0.0583376	-0.0586125	-0.0586180	-0.0586181	-0.0586181	-0.0586181
4.80	0	-0.0569192	-0.0577836	-0.0578316	-0.0578365	-0.0578395	-0.0578398
4.88		-0.0572647	-0.0579469	-0.0579775	-0.0579797	-0.0579805	-0.0579809
4.96		-0.0575664	-0.0581076	-0.0581273	-0.0581283	-0.0581286	-0.0581286
5.04		-0.0578392	-0.0582705	-0.0582834	-0.0582838	-0.0582839	-0.0582839
5.12		-0.0580941	-0.0584393	-0.0584478	-0.0584480	-0.0584480	-0.0584480
5.20		-0.0583392	-0.0586167	-0.0586224	-0.0586225	-0.0586225	-0.0586225
4.80	0.05	-0.0569329	-0.0577875	-0.0578335	-0.0578378	-0.0578398	-0.0578382
4.88		-0.0572725	-0.0579474	-0.0579767	-0.0579787	-0.0579792	-0.0579791
4.96		-0.0575711	-0.0581066	-0.0581256	-0.0581265	-0.0581267	-0.0581267
5.04		-0.0578418	-0.0582688	-0.0582812	-0.0582816	-0.0582817	-0.0582817
5.12		-0.0580948	-0.0584367	-0.0584449	-0.0584451	-0.0584451	-0.0584451
5.20		-0.0583376	-0.0586125	-0.0586180	-0.0586181	-0.0586181	-0.0586181
4.80	0.10	-0.0569667	-0.0577922	-0.0578323	-0.0578348	-0.0578347	-0.0578333
4.88		-0.0572943	-0.0579470	-0.0579729	-0.0579741	-0.0579741	-0.0579738
4.96		-0.0575848	-0.0581035	-0.0581204	-0.0581209	-0.0581209	-0.0581209
5.04		-0.0578497	-0.0582638	-0.0582749	-0.0582752	-0.0582752	-0.0582752
5.12		-0.0580979	-0.0584299	-0.0584373	-0.0584375	-0.0584375	-0.0584375
5.20		-0.0583363	-0.0586036	-0.0586086	-0.0586086	-0.0586086	-0.0586086

Table 3
The Same Comparison as in Tables 1 and 2, but for the Disk with $2l = 4$, $m = 1$ (Top Table) and $2l = 6$, $m = 1$ (Bottom Table)

$m = 1, 2l = 4$		Number of Summed Terms					Exact
ρ	z	5	10	20	30	50	
4.80	-0.10	-0.0909074	-0.0936320	-0.0945185	-0.0947409	-0.0946453	-0.0942394
4.88		-0.0922746	-0.0943892	-0.0949413	-0.0950419	-0.0950309	-0.0949059
4.96		-0.0936211	-0.0952718	-0.0956207	-0.0956669	-0.0956675	-0.0956439
5.04		-0.0949235	-0.0962192	-0.0964426	-0.0964643	-0.0964654	-0.0964624
5.12		-0.0961652	-0.0971877	-0.0973326	-0.0973429	-0.0973435	-0.0973431
5.20		-0.0973348	-0.0981457	-0.0982408	-0.0982458	-0.0982461	-0.0982460
4.80	-0.05	-0.0904014	-0.0932407	-0.0942827	-0.0946795	-0.0951708	-0.0942827
4.88		-0.0919799	-0.0941792	-0.0948207	-0.0949929	-0.0951267	-0.0949623
4.96		-0.0935060	-0.0952196	-0.0956208	-0.0956972	-0.0957356	-0.0957267
5.04		-0.0949607	-0.0963035	-0.0965581	-0.0965927	-0.0966042	-0.0966051
5.12		-0.0963312	-0.0973892	-0.0975529	-0.0975689	-0.0975725	-0.0975727
5.20		-0.0976094	-0.0984472	-0.0985539	-0.0985614	-0.0985626	-0.0985627
4.80	0	-0.0898955	-0.0927735	-0.0938696	-0.0943315	-0.0950867	-0.0942974
4.88		-0.0916961	-0.0939239	-0.0945965	-0.0947952	-0.0949925	-0.0949818
4.96		-0.0934096	-0.0951445	-0.0955638	-0.0956512	-0.0957058	-0.0957578
5.04		-0.0950222	-0.0963809	-0.0966463	-0.0966855	-0.0967015	-0.0967061
5.12		-0.0965254	-0.0975953	-0.0977655	-0.0977836	-0.0977884	-0.0977890
5.20		-0.0979147	-0.0987615	-0.0988722	-0.0988806	-0.0988822	-0.0988823
4.80	0.05	-0.0904014	-0.0932407	-0.0942827	-0.0946795	-0.0951708	-0.0942827
4.88		-0.0919799	-0.0941792	-0.0948207	-0.0949929	-0.0951267	-0.0949623
4.96		-0.0935060	-0.0952196	-0.0956208	-0.0956972	-0.0957356	-0.0957267
5.04		-0.0949607	-0.0963035	-0.0965581	-0.0965927	-0.0966042	-0.0966051
5.12		-0.0963312	-0.0973892	-0.0975529	-0.0975689	-0.0975725	-0.0975727
5.20		-0.0976094	-0.0984472	-0.0985539	-0.0985614	-0.0985626	-0.0985627
4.80	0.10	-0.0909074	-0.0936320	-0.0945185	-0.0947409	-0.0946453	-0.0942394
4.88		-0.0922746	-0.0943892	-0.0949413	-0.0950419	-0.0950309	-0.0949059
4.96		-0.0936211	-0.0952718	-0.0956207	-0.0956669	-0.0956675	-0.0956439
5.04		-0.0949235	-0.0962192	-0.0964426	-0.0964643	-0.0964654	-0.0964624
5.12		-0.0961652	-0.0971877	-0.0973326	-0.0973429	-0.0973435	-0.0973431
5.20		-0.0973348	-0.0981457	-0.0982408	-0.0982458	-0.0982461	-0.0982460
$m = 1, 2l = 6$		Number of Summed Terms					Exact
ρ	z	5	10	20	30	50	
4.80	-0.10	-0.0940721	-0.0990223	-0.1003870	-0.1007140	-0.1005770	-0.0999929
4.88		-0.0961241	-0.0999771	-0.1008290	-0.1009760	-0.1009610	-0.1007820
4.96		-0.0980710	-0.1010870	-0.1016260	-0.1016940	-0.1016950	-0.1016610
5.04		-0.0998925	-0.1022660	-0.1026120	-0.1026440	-0.1026450	-0.1026410
5.12		-0.1015770	-0.1034550	-0.1036790	-0.1036940	-0.1036950	-0.1036950
5.20		-0.1031180	-0.1046110	-0.1047580	-0.1047660	-0.1047660	-0.1047660
4.80	-0.05	-0.0932709	-0.0984244	-0.1000260	-0.1006080	-0.1013160	-0.1000470
4.88		-0.0956494	-0.0996529	-0.1006410	-0.1008940	-0.1010870	-0.1008530
4.96		-0.0978652	-0.1009940	-0.1016130	-0.1017250	-0.1017800	-0.1017680
5.04		-0.0999080	-0.1023660	-0.1027600	-0.1028100	-0.1028270	-0.1028280
5.12		-0.1017740	-0.1037150	-0.1039690	-0.1039920	-0.1039970	-0.1039980
5.20		-0.1034630	-0.1050040	-0.1051690	-0.1051810	-0.1051820	-0.1051820
4.80	0	-0.0925102	-0.0977323	-0.0994168	-0.1000940	-0.1011800	-0.1000650
4.88		-0.0952238	-0.0992782	-0.1003140	-0.1006050	-0.1008890	-0.1008780
4.96		-0.0977140	-0.1008800	-0.1015270	-0.1016550	-0.1017340	-0.1018080
5.04		-0.0999807	-0.1024670	-0.1028770	-0.1029350	-0.1029580	-0.1029640
5.12		-0.1020290	-0.1039910	-0.1042550	-0.1042820	-0.1042890	-0.1042890
5.20		-0.1038650	-0.1054230	-0.1055950	-0.1056070	-0.1056090	-0.1056090
4.80	0.05	-0.0932709	-0.0984244	-0.1000260	-0.1006080	-0.1013160	-0.1000470
4.88		-0.0956494	-0.0996529	-0.1006410	-0.1008940	-0.1010870	-0.1008530
4.96		-0.0978652	-0.1009940	-0.1016130	-0.1017250	-0.1017800	-0.1017680
5.04		-0.0999080	-0.1023660	-0.1027600	-0.1028100	-0.1028270	-0.1028280
5.12		-0.1017740	-0.1037150	-0.1039690	-0.1039920	-0.1039970	-0.1039980
5.20		-0.1034630	-0.1050040	-0.1051690	-0.1051810	-0.1051820	-0.1051820
4.80	0.10	-0.0940721	-0.0990223	-0.1003870	-0.1007140	-0.1005770	-0.0999929
4.88		-0.0961241	-0.0999771	-0.1008290	-0.1009760	-0.1009610	-0.1007820
4.96		-0.0980710	-0.1010870	-0.1016260	-0.1016940	-0.1016950	-0.1016610
5.04		-0.0998925	-0.1022660	-0.1026120	-0.1026440	-0.1026450	-0.1026410
5.12		-0.1015770	-0.1034550	-0.1036790	-0.1036940	-0.1036950	-0.1036950
5.20		-0.1031180	-0.1046110	-0.1047580	-0.1047660	-0.1047660	-0.1047660

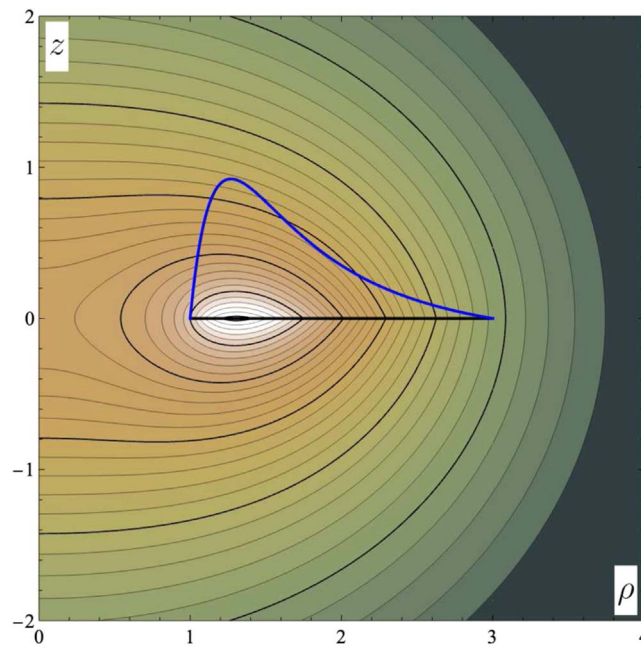


Figure 1. Meridional-plane contour plot of potential (58) of the disk with compact support at ($\rho_{\text{in}} = \mathcal{M}$, $\rho_{\text{out}} = 3\mathcal{M}$). The disk is indicated by the black line, and the corresponding density profile (57) is inserted into the plot by the thick blue line. The potential value ranges from -0.285 (dark green) to -0.846 (white). The values at the axes are in the units of \mathcal{M} .

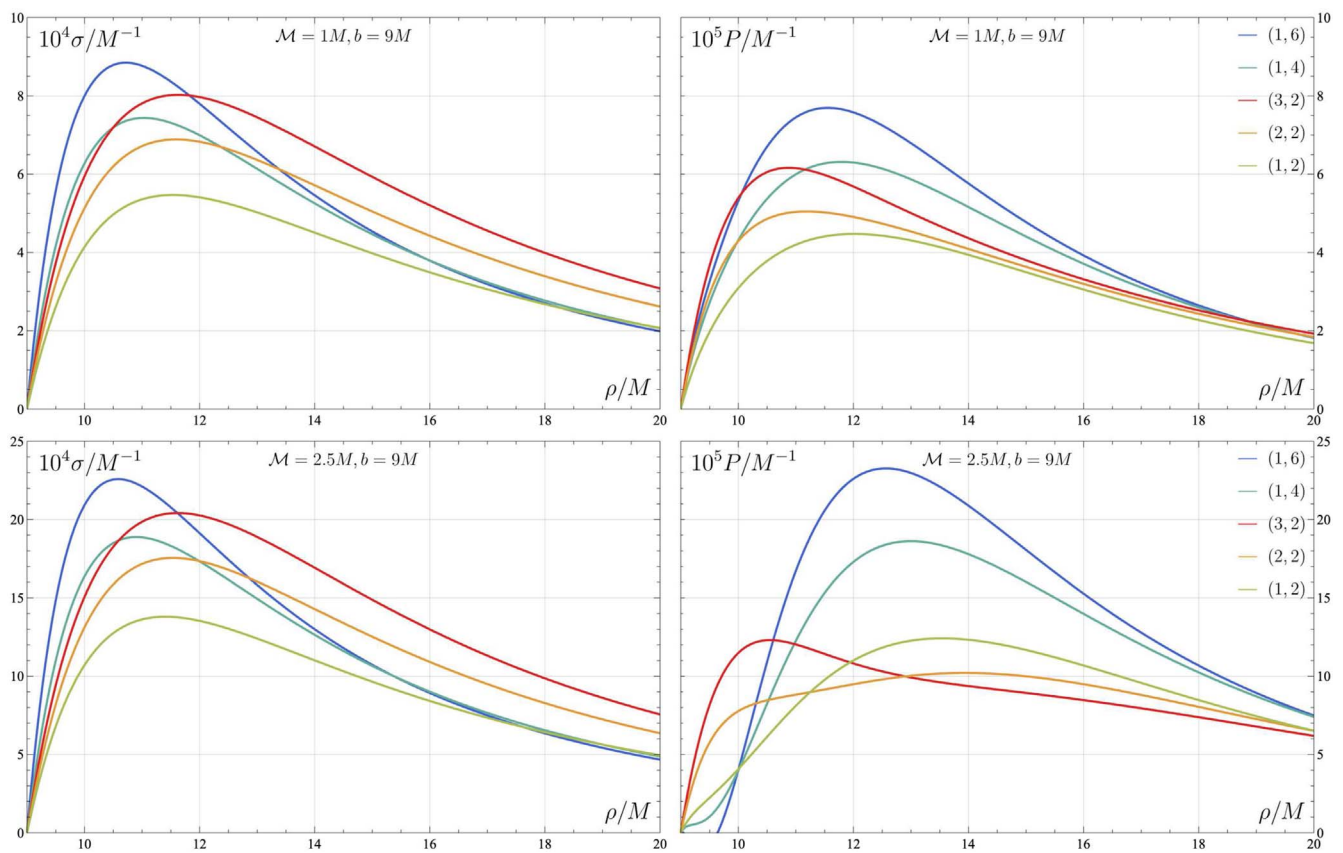


Figure 2. Radial profiles of the surface density σ (left column) and of azimuthal pressure P (right column), as measured by local static observers, are plotted for several disks of the infinite annular type ($\rho \geq b$)—i.e., those generating potentials (53)—encircling a Schwarzschild black hole (of mass M). Basic parameters are given in the plots, with different $(m, 2l)$ cases distinguished by color.

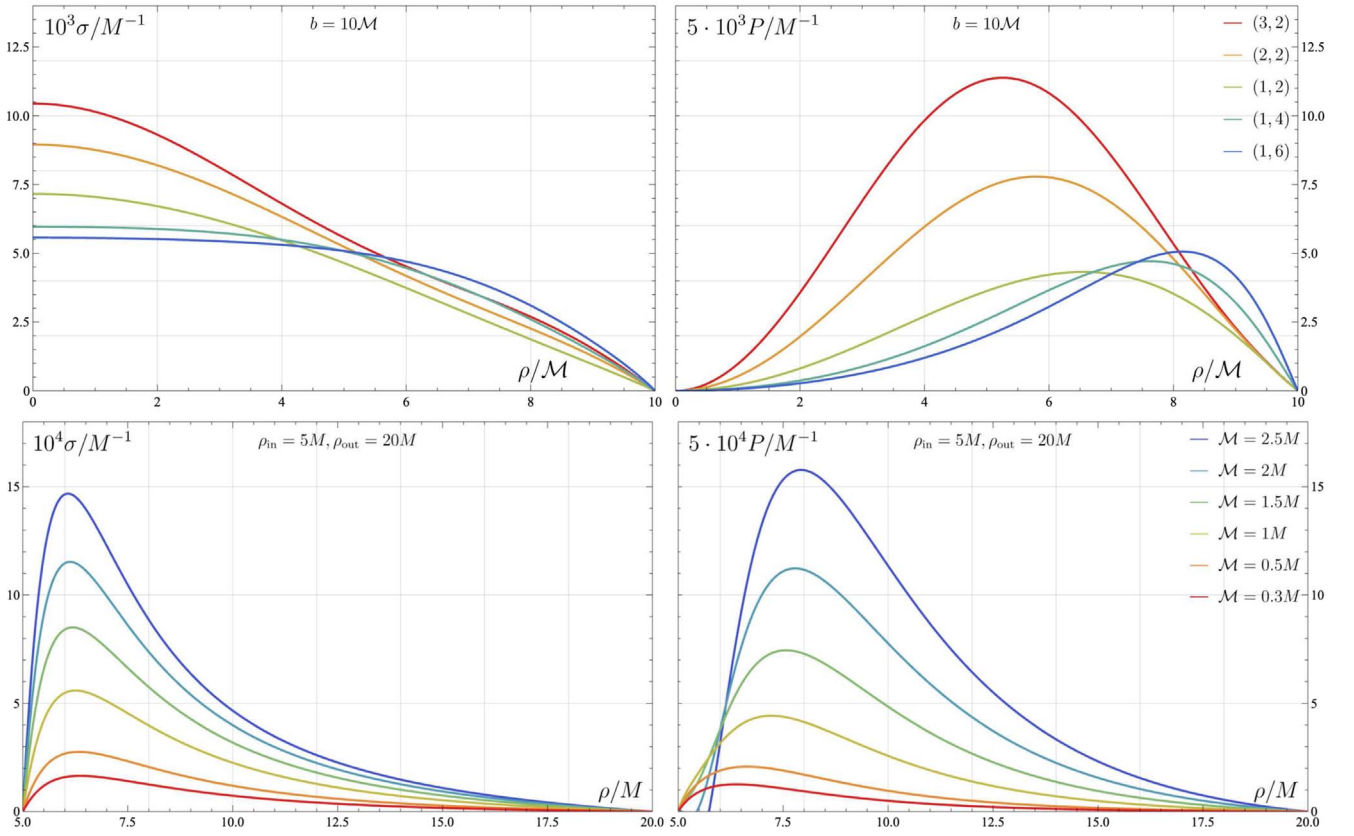


Figure 3. Radial profiles of the surface density σ (left column) and of azimuthal pressure P (right column), as measured by local static observers, are plotted for several solid disks ($\rho \leq b$) with potentials (43) (top row), and for several finite annular disks ($\rho_{\text{in}} \leq \rho \leq \rho_{\text{out}}$) with potentials (58) with a Schwarzschild black hole at their center (bottom row). Basic parameters are given in the plots, M is the black hole mass, and the different cases $(m, 2l)$ are distinguished by color.

and demands that

$$w(\rho' = \rho_{\text{in}}) = 0, \quad w(\rho' = \rho_{\text{out}}) = 0, \quad \text{while } w(\rho') > 0 \text{ for } \rho_{\text{in}} < \rho' < \rho_{\text{out}}.$$

For $L = 1$ (preceding paragraph), there are two parameters (W_{-3} and W_{-5}) and two constraints, so no parameters are left free (besides the overall scaling, as determined by \mathcal{M} through W_0). For $L = 2$, the density contains three parameters (W_{-3} , W_{-5} , and W_{-7}), which again are bound by two constraints, so one of them effectively remains free. In general, $L - 1$ of the W parameters only remain restricted by condition that the density must not have any root *inside* the radial range of the disk.

8. Radial Profiles of Density and of Azimuthal Pressure

Two simple types of physical interpretation of the disk sources involve: (i) a single-component ideal fluid with a certain surface density (σ) and an azimuthal pressure (P), which keeps the orbits at their radius; or (ii) two identical counter-orbiting dust components with proper surface densities $\sigma_+ = \sigma_-$ following circular geodesics with equal but opposite velocities relative to static observers, $v_+ = -v_-$ (see, e.g., González & Espitia 2003). In Figure 2, we show the radial profiles of surface density σ and of azimuthal pressure P ,⁶

$$\sigma = \frac{\nu_{,z}(z = 0^+)}{2\pi} (1 - \rho\nu_{,\rho}), \quad P = \frac{\nu_{,z}(z = 0^+)}{2\pi} \rho\nu_{,\rho},$$

for several annular disks encircling a Schwarzschild black hole. Figure 3 illustrates the same parameters for several solid and several bump-type disks. Some curves are seen to fall below zero around the inner disk edge, which means such orbits (understood as hoops) would have to be in a state of tension in order to stay at their respective radii, i.e., they are attracted outward rather than downward, due to a “too large” mass of the disk at larger radii. Such a circumstance corresponds to when free circular motion is impossible (see the following section).

⁶ Quantities defined in this way sum to $w \equiv \sigma + P = \nu_{,z}(z = 0^+)/2\pi$, and exactly this sum satisfies the Poisson equation $\nabla^2\nu = 4\pi w(\rho)\delta(z)$, so it is the counterpart of Newtonian density.

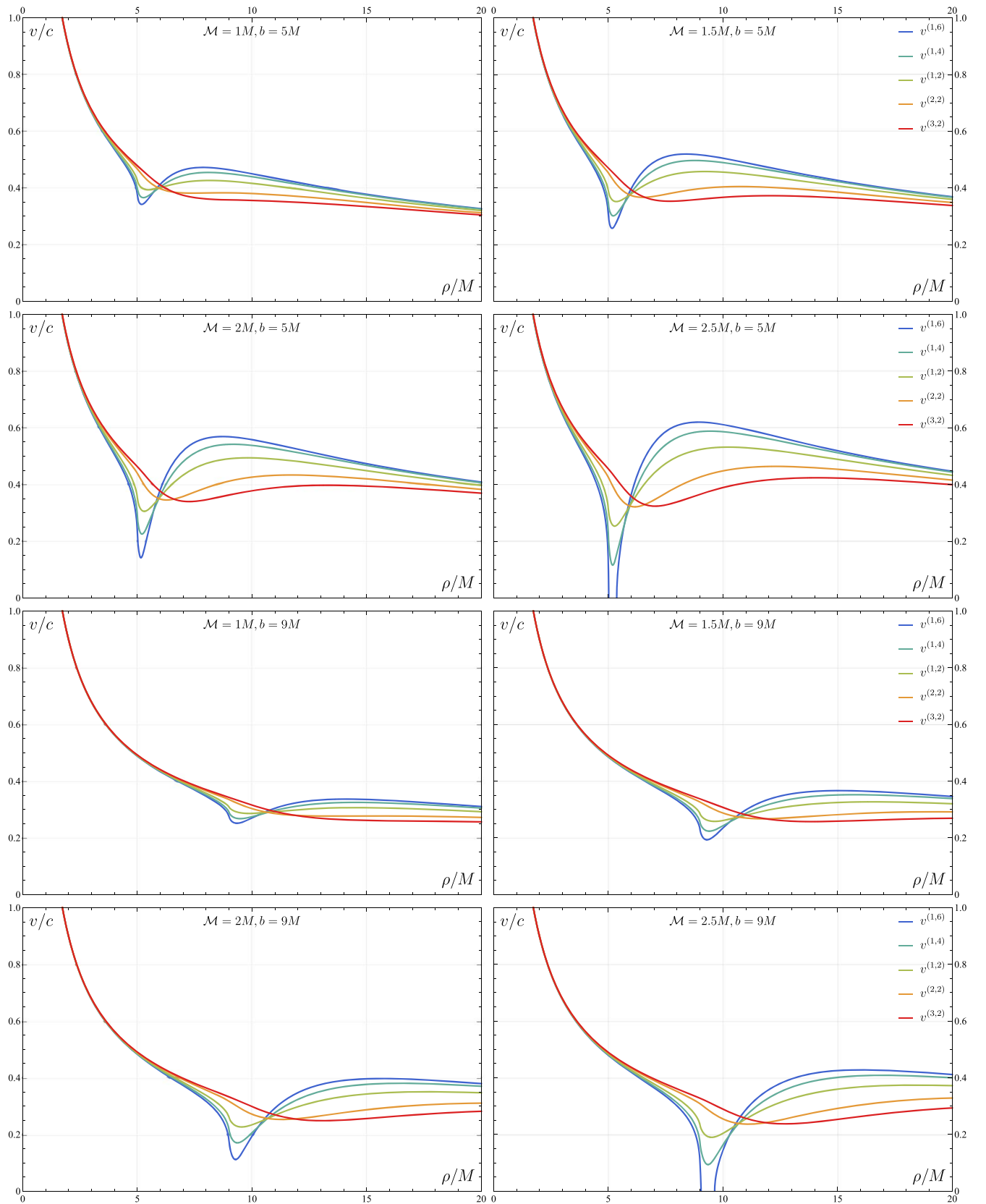


Figure 4. Radial profiles of circular-geodesic speeds as measured by local static observers, $v^{(m,2l)}$, plotted for a Schwarzschild black hole (of mass M) encircled by several disks of the annular type ($\rho \geq b$), i.e., those generating potentials (53). Basic parameters are given in the plots.

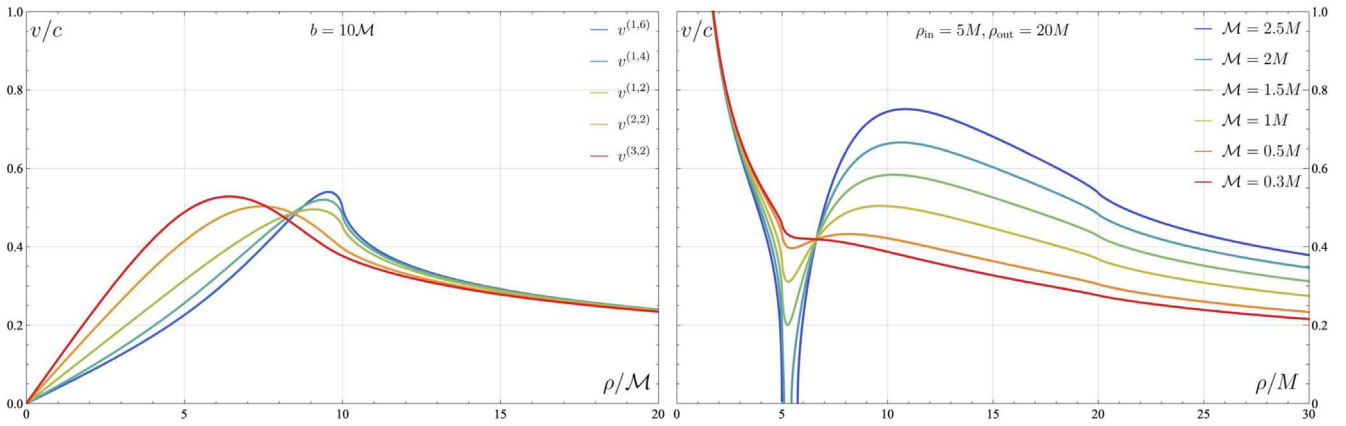


Figure 5. Radial profiles of circular-geodesic speeds relative to local static observers, plotted for several solid disks ($\rho \leq b$) with potentials (43) ($v^{(m,2)}$, left), and for several finite annular disks ($\rho_{\text{in}} \leq \rho \leq \rho_{\text{out}}$) with potentials (58) with a Schwarzschild black hole at their center (right). Basic parameters are given in the plots, and M is the black hole mass.

9. Circular-velocity Profiles

One of useful illustrations of an axisymmetric-source field possessing a plane with respect to which it is reflection symmetric, at least locally (it is called the equatorial plane), is the radial profile of circular velocity, i.e., of the velocity corresponding to free circular orbits of test particles. In the Weyl-type spacetimes, such a (linear) velocity, measured by a static observer at the given radius, is given by

$$v_{\pm}^2 \equiv v_{\pm}^2 =: v^2 = \frac{P}{\sigma} = \frac{\rho v_{,\rho}}{1 - \rho v_{,\rho}}.$$

We show how the rotation profile appears for the above disk sources in Figures 4 (annular disks around a black hole) and 5 (solid disk without a black hole, and finite “bump”-type disk with a black hole). Since the equatorial plane in this case coincides with that of the disks, the profiles tell, at the same time, where it is possible to interpret the disk in terms of two identical counter-orbiting geodesic streams. In the figures, several occasions can be seen where the disk is so heavy that it is not possible to orbit freely below its maximum (even a particle at rest is attracted outward to the disk, despite the opposite effect of the black hole).

10. Concluding Remarks

We have computed in closed form the potential of static thin circular disks with density given by a power law in radius, employing the method suggested by Conway (2000). Starting with the contribution of the elementary density terms $(\rho')^{2l}$ (for solid disks) and $(\rho')^{-3-2l}$ (for annular disks reached by inversion), we wrote down the potential due to a generic static thin circular disk whose density involves even powers of density. The results are expressed in terms of elliptic integrals multiplied by polynomials, which can readily be found using Mathematica or a similar program.⁷ All the results are exact solutions of Einstein field equations (belonging to the Weyl class of static and axisymmetric spacetimes). The annular disks resulting from inversion with respect to the rim are infinite (yet with finite mass), but finite disks can easily be obtained as well by suitable superposition of the basic density terms. We performed a numerical check of the results against Legendre-series expansion, which we used to solve the problem in the past (Semerák 2004). We also illustrated the results on the radial profiles of basic physical parameters of the disks.

Finally, let us mention several closely related results from the literature. In astrophysics, disk sources are constantly under study. This is particularly true in galactic dynamics, but also in relativistic astrophysics where accretion disks encircling compact objects are central to the physics of active galactic nuclei and of X-ray binaries. However, in the latter case, it is rather rare that the disk-source gravity is incorporated in an *exact* way. From the time we were interested in the problem in the 2000s, new exact analytical results on thin disks have been obtained by Huré and collaborators, in particular by employing their semi-analytical method of tackling the singularity of the Green function necessarily occurring inside the source (Huré & Pierens 2005)—see, e.g., Huré et al. (2007) for thus computed potentials of power-law thin disks. Schulz (2009) gave exact analytical solutions for the first three disks of what in general relativity is known as the counter-rotating Morgan–Morgan static thin disk family (Morgan & Morgan 1969), which we referred to in Section 2. He also (Schulz 2012) found the exact closed-form potential and field of the Mestel finite disk (it is the one for which the circular velocity is constant). Vogt & Letelier (2009) obtained new thin-disk solutions via special superpositions within the Kuzmin–Toomre disk family. A new family of thin disks was also presented by González et al. (2009), but Gleiser (2012) showed that the properties of these solutions are rather unsatisfactory. More physical results seem to have been obtained recently by Vieira (2020) via the “displace, cut, and reflect” method applied to multi-black-hole solutions (which appear as N collinear rods located on the symmetry axis in the Weyl coordinates).

⁷ However, algorithms that we have found in the literature either aim at *numerical* evaluation of the integrals (16), or they involve *spherical* Bessel functions $j_j(x) = \sqrt{\frac{\pi}{2x}} J_{j+1/2}(x)$

We are thankful for support from grant GACR 21-11268S of the Czech Science Foundation (D.K., O.S.) and from grant schemes at Charles University, reg. No. CZ.02.2.69/0.0/0.0/19_073/0016935 (P.K.).

ORCID iDs

O. Semerák  <https://orcid.org/0000-0002-1272-6779>

References

- Bičák, J., Lynden-Bell, D., & Katz, J. 1993, *PhRvD*, 47, 4334
 Conway, J. T. 2000, *MNRAS*, 316, 540
 Conway, J. T. 2001, *ITM*, 37, 2977
 Eason, G., Noble, B., & Sneddon, I. N. 1955, *RSPTA*, 247, 529
 Gleiser, R. J. 2012, *PhRvD*, 85, 028501
 González, G. A., & Espitia, O. A. 2003, *PhRvD*, 68, 104028
 González, G. A., Gutiérrez-Piñeres, A. C., & Viña-Cervantes, V. M. 2009, *PhRvD*, 79, 124048
 Hanson, M. T., & Puja, I. W. 1997, *QApMa*, 55, 505
 Huré, J.-M., Pelat, D., & Pierens, A. 2007, *A&A*, 475, 401
 Huré, J.-M., & Pierens, A. 2005, *ApJ*, 624, 289
 Kausel, E., & Baig, M. M. I. 2012, *QApMa*, 70, 77
 Lass, H., & Blitzer, L. 1983, *CeMec*, 30, 225
 Lemos, J. P. S., & Letelier, P. S. 1994, *PhRvD*, 49, 5135
 Morgan, T., & Morgan, L. 1969, *PhRv*, 183, 1097, (Errata: 1969, *PhRv*, 188, 2544; 1970, *PhRvD*, 1, 3522)
 Schulz, E. 2009, *ApJ*, 693, 1310, (Erratum: 2018, *ApJ*, 857, 75)
 Schulz, E. 2012, *ApJ*, 747, 106
 Semerák, O. 2003, *CQGra*, 20, 1613
 Semerák, O. 2004, *CQGra*, 21, 2203
 Toomre, A. 1963, *ApJ*, 138, 385
 Vieira, R. S. S. 2020, *CQGra*, 37, 205013
 Vogt, D., & Letelier, P. S. 2009, *MNRAS*, 396, 1487